Range-based rail gauge and rail fasteners detection using high-resolution 2D/3D images

Alejandro García Lorente
Graduate Research Assistant
Computer Engineering Department
Polytechnic School, University of Alcalá - 28871 Alcalá de Henares (Madrid, Spain)
Phone: (0034) 91-8856702
Email: alejandro.glorente@gmail.com

David Fernández Llorca
Associate Professor
Computer Engineering Department
Polytechnic School, University of Alcalá - 28871 Alcalá de Henares (Madrid, Spain)
Phone: (0034) 91-8856682
Email: david.fernandezl@uah.es

Miguel Gavilán Velasco (corresponding author)
Head of R&D Division
Euroconsult Group
Avda. Montes de Oca, 9-11, P. I. Sur - 28703. S. S. De los Reyes (Madrid, Spain)
Phone: (0034) 91-6597831
Email: mgavilan@euroconsult-group.com

José Antonio Ramos García
New Technologies Director
Euroconsult Group
Avda. Montes de Oca, 9-11, P. I. Sur - 28703. S. S. De los Reyes (Madrid, Spain)
Phone: (0034) 91-6597831
Email: jramosg@euroconsult-group.com

Fernando Sánchez Domínguez
R&D Director
Euroconsult Group
Avda. Montes de Oca, 9-11, P. I. Sur - 28703. S. S. De los Reyes (Madrid, Spain)
Phone: (0034) 91-6597831
Email: mgavilan@euroconsult-group.com

Submission Date: 07/31/2013
Word Count: 3770
Tables and Figures: 14*250= 2500
Total Words: 6270

ABSTRACT

Defects in railroad tracks are responsible for several incidents every year. Rail gauge is the most important measurement for track maintenance, because deviations in gauge indicate where potential defects may exist. In addition, missing rail fasteners can be considered as a critical defect that should be detected and repaired. In this paper, an automatic inspection system specifically devised to estimate the rail gauge and detect missing rail fasteners is presented. A 3D imaging sensor, which produces high-resolution 2D images and 3D profiles, is used to capture the data. Then a range-based approach is used to inspect the railroad track. We rely on the 3D structure of the rail components (rail heads and rail fasteners) instead of using a vision-based approach which suffers from illumination changes. The system is evaluated using data recorded from real scenarios in two different cities (Metro Madrid and London Underground), with different nominal gauge values and fastening elements. The system is described and results are presented, evaluated and discussed.

KEYWORDS: rail gauge detection, rail fasteners detection, rail track inspection, 3D point clouds analysis.

INTRODUCTION

Defects in railroad tracks are responsible for several incidents every year resulting in fatalities, injuries, extensive material damage, environmental damage (dangerous goods), etc. According to Federal Railroad Administration's (FRA) Office of Safety Analysis, the 32% of the train accidents in the United States from the decade 2000-2010 occurred due to defects in the tracks *(1)*. Although in the European Union most of the fatalities are caused by railway suicides, rolling stock in motion, and level-crossing accidents, on average, a derailment or a collision is reported at least every second day in the European Union *(2)*. Most of the derailment accidents and collisions are also due to defects in the tracks and they are usually categorized as serious accidents into which National safety authorities mostly decide to open an investigation. Accordingly, efficient inspection and maintenance of railroad tracks are fundamental tasks that should be carried out on a regular basis. Human inspectors are usually the main actors when performing track inspection. Although their efforts are very thorough, the manual inspection process can be extremely tedious, demanding and time-consuming. An automatic inspection system able to identify railroad track defects will therefore be a valuable tool to improve the efficiency of current inspection procedures. Track defects can be classified into two main categories: (i) Track Geometry, which includes deviation from the nominal gauge measure, misalignment, etc.; (ii) Track Structure, which includes defects and missing parts in the tie-plates, fasteners, bolts, etc.

The main goal of the proposed work is to present a new non-contact-type railroad track inspection system by means of a 3D imaging sensor which produces high-resolution 2D images and 3D profiles. The data supplied by the sensor is analyzed using intelligent 3D processing techniques, focusing in two main objectives: track gauge monitoring and missing rail-fasteners detection. On the one hand, rail gauge is obtained by analyzing the 3D cross-sectional profile with a resolution of 1 millimeter. Rail heads are firstly detected and the limits of the inner faces are refined by searching the points that appears at a certain distance below the rail head. On the other hand, missing fasteners detection is carried out using a generic two-staged approach that combines localization and verification.

The proposed range-based railroad track inspection system described in this paper was developed through an interdisciplinary research collaboration between the company EUROCONSULT GROUP (Madrid, Spain) and the Innovative Sensing and Intelligent Systems (ISIS) research group at the University of Alcalá (UAH, Alcalá de Henares, Spain).

RELATED WORK

There is extensive literature on automatic inspection of railroad track and track components. Inspection technologies are usually installed on board of track geometry cars, including computers to process and display data gathered by the systems. Although contact measurement systems exist, they can be considered as obsolete since most of the measurement devices are now based on non-contact sensors. Well established inspection techniques such as ultrasonic rail flaw, geometry car testing, inertial accelerometers, etc., were surveyed in *(3)*. The authors stated that machine vision is the most applicable technology given the manual, visual nature of old track inspections. As a matter of fact, machine vision approaches to assist rail track inspection has attracted much interest in the last years from both industry and research groups at Universities.

A track simulation model used to evaluate camera views and to provide synthetic images for machine vision algorithm development was proposed by the Computer Vision and

Robotics Laboratory (CVRL) at the University of Illinois in *(3)*. Cameras are finally placed laterally to obtain lateral views of track components. The inspection algorithm follows a global-to-local scheme, with the most consistent detectable objects being located first (ballast, rail, ties) followed by smaller components (tie plates, spikes and anchors). Using edge detection and texture information, the same group presents a robust means of detecting rail, ties and ties plates *(4)*, which narrows again the search area. Then, prior knowledge of probable component locations is applied to determine the presence of spikes and rail anchors. In a most recent works *(5)*, *(6)*, special track components are periodically inspected to detect turnouts.

The Exploratory Computer Vision Group (ECVG) at Watson Research Center developed a vision-based track condition monitoring system *(7)*, *(8)*, able to detect different rail components such as spikes, anchors, tie plates and bolts. Hough transform plays here a very important role, since it is used to locate both tie plates (lines) and spikes (ellipses). Spike holes and anchors are detected by analyzing edges distribution. The system is evaluated using their own dataset, resulting in an average detection rate of 98.2%. The authors remark the high variability of track components appearance that comes from diversities in components (anchor, tie plate, spikes, etc.) type, size, shape, camera view point, occlusion and light condition.

In *(9)* and *(10)*, the Computer Vision Lab at University of Central Florida, proposed the use of SIFT features combined with MACH filters and SVM to detect both rail fasteners and missing rail fasteners. Rail fasteners hold the steel rail to the perpendicular crossties. Since these ones can take several geometries and can differ depending upon their purpose and producer, the problem is addressed as a multi-classification problem. Up to seven classes are used including steel clips, E-clips, missing, defective, etc. Lighting variance is mitigated by using normalized correlation filters.

Considering the detection of the rail gauge, in *(9)* and *(10)*, two approaches are presented: pure laser and pure camera. Vision-based approach makes use of the Hough transform to detect persistent edge lines and validate the rail limits. Laser-based approach applies a 3-means clustering technique to isolate the rail head. The rail head surface is then approximated by a third degree polynomial, and inner rail edge points are obtained by computing the intersection of a vertical plane tangent to the rail head surface. Finally, rail gauge is calculated using the distance between matching edge points. Although the methods are well explained, the evaluation is poor since no comparisons are given with respect to a specific ground truth.

In the context of the industry, various commercial systems are available for performing rail track inspection. Examples include the AURORA system for inspecting wood ties, rail seat abrasion, tie plates, anchors and spikes *(11)*. ENSCO developed the *VisiRail*^{TM} Joint Bar Inspection System, using high-resolution scan line cameras and laser sensors *(12)*. High-speed line-scan cameras are also used by the system developed by MERMEC Group to detect track surface defects and measures track geometry, rail profile and rail corrugation *(13)*. Finally, the TrackVue system *(14)*, developed by RailVision, is applied for measuring rail wear, track gauge and curvature, rail cant and vegetation cover, etc., using an array of cameras and laser equipment. It is worth to mention that with commercial systems, neither technical details nor performance reports are available, so it is very complicated to establish their performance in the context of some reference baseline.

In this paper, a range-based rail track inspection system is presented. The nature of our data does not suffer from illumination changes as it happens with machine vision algorithms. We rely on the 3D structure of the rail components (rail heads and rail fasteners) to obtain two main measurements: track gauge and missing rail fasteners. The system is evaluated using data recorded from real scenarios in different countries, with different nominal gauge values and fastening systems. The system is described and results are presented, evaluated and discussed.

SYSTEM DESCRIPTION

The proposed rail track inspection system can be defined by three main blocks, depicted in Figure 1. The measurement device is composed of a set of sensors including an odometer, an Inertial Measurement Unit (IMU) and the laser and scan line camera system. The sensors are connected to a PC which is responsible for recording all the data provided by the sensors. On-line processing is not a critical point for this application. Accordingly, the procedure was designed to store all the data in a set of data storage devices that will be used as the input of the off-line processing system.

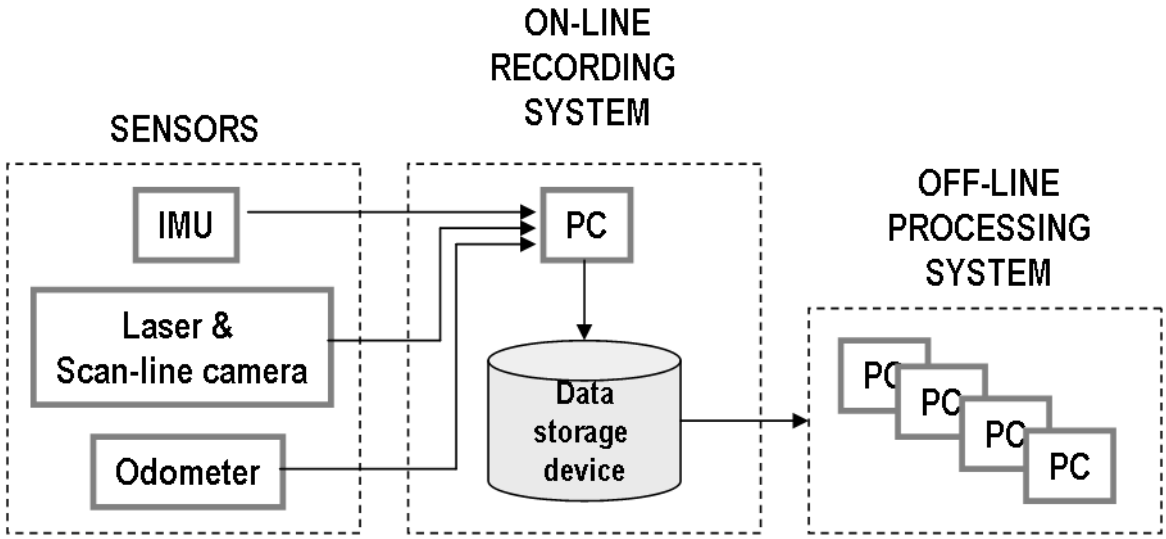

FIGURE 1 System overview

Measurement Device

The main component of the measurement block is the high-speed laser scanner *(15)* that provides both 2D images and high-resolution 3D profiles of the railroad track (see Figure 2 –right-). It can scan at 1-mm image resolution and 3D data at acquisition speeds between 0-50 km/h. The platform used to storage the data is integrated in a global system devised for tunnel inspection (see Figure 2 –left-). The acquisition software makes use of the data provided by the laser scanner, the IMU and the odometer to finally storage a 3D cloud of points with appearance information coming from the scan line camera. A couple of examples of the data supplied by our sensor are shown in Figure 3. As can be observed, the level of detail is very rich. All the track components (rail heads, fastening systems, tails, etc.) are perfectly visible and distinguishable.

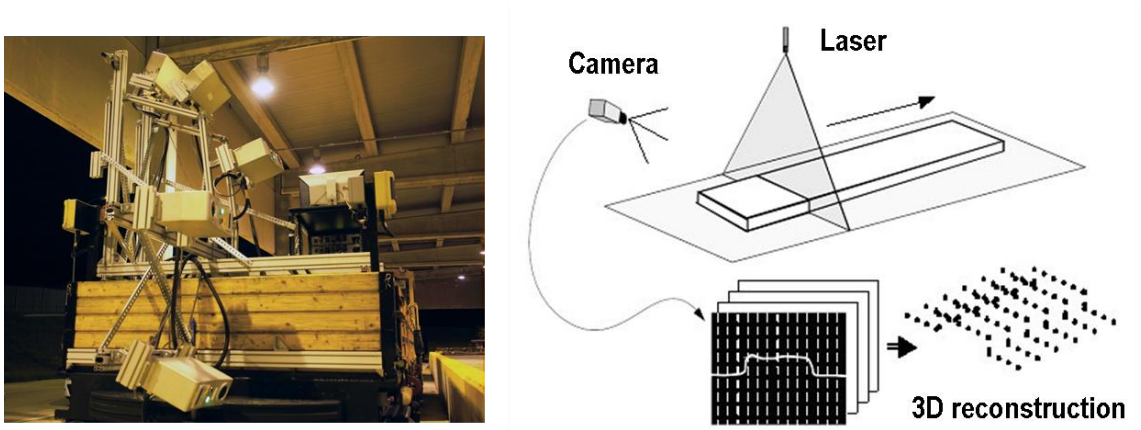

FIGURE 2 Left: tunnel/rail track inspection platform. Right: sensor overview.

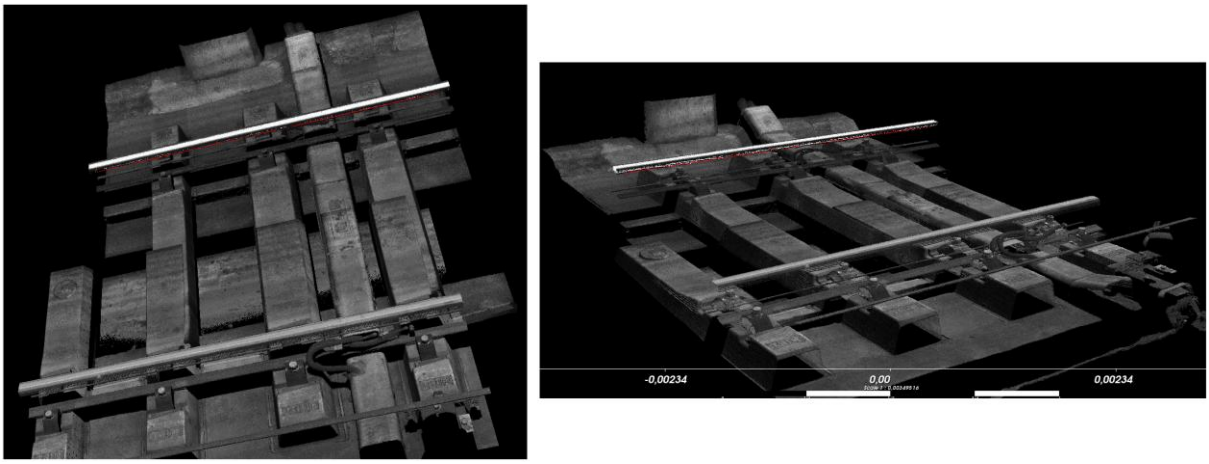

FIGURE 3 Data supplied by the high-speed laser scanner and scan line camera.

Track gauge detection

The proposed approach used to estimate the rail gauge is depicted in Figure 4. The 3D cloud of points is divided into horizontal scan-lines that are evaluated independently. In order to detect the main changes (edges) of the scan-line profile we use the Derivative of Gaussian (DoG) function. The DoG allows edge detection in only one step in the context of noise. An example of the DoG applied in a single scan-line that corresponds to one rail is depicted in Figure 5.

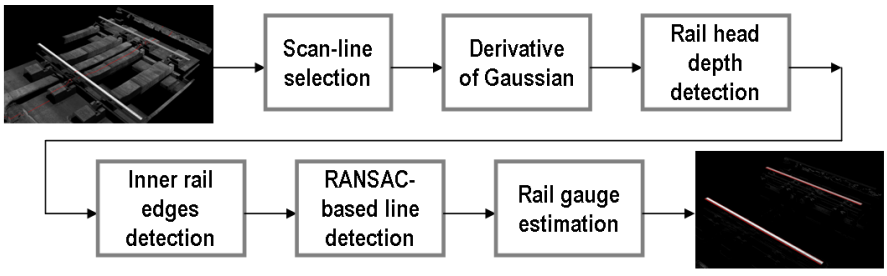

FIGURE 4 Overview of the rail gauge detection procedure.

In order to detect the inner rail edges, we use the definition of rail gauge, which is computed with respect to the two inner points of both rails, defined 14mm below each rail

head top. Accordingly, the first step consists in computing the rail head depth. As can be observed in Figure 5, the rail head boundaries produce a maximum and a minimum in the DoG function. By searching this specific pattern (maximum and minimum) and introducing a depth restriction (rail head is considered the closer region with respect to the sensor), the rail head limits are finally obtained. The depth of the rail head is computed as the mode value between those boundaries. Then, inner rail edges are estimated by selecting the inner point that appears at 14mm below the rail head depth. A linear interpolation is applied when no point appears at this exact position with respect to the rail head depth. An example of this procedure is depicted in Figure 6.

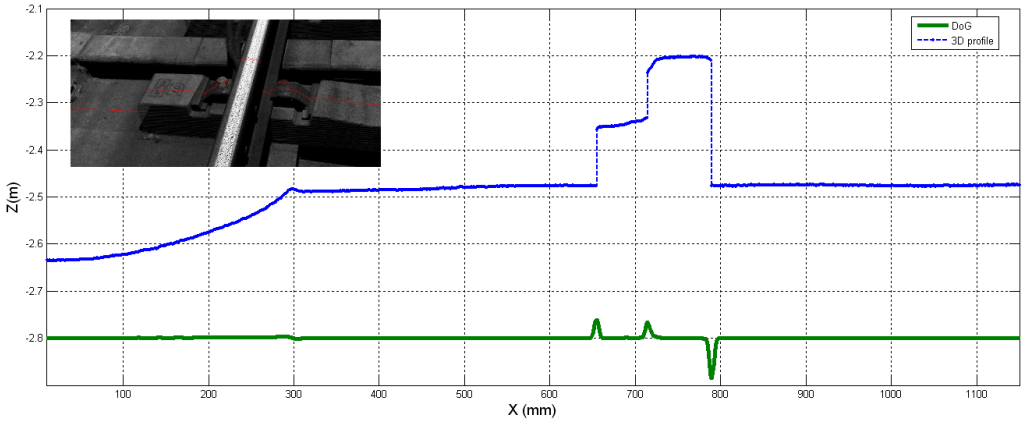

FIGURE 5 Scan-line 3D profile and DoG result.

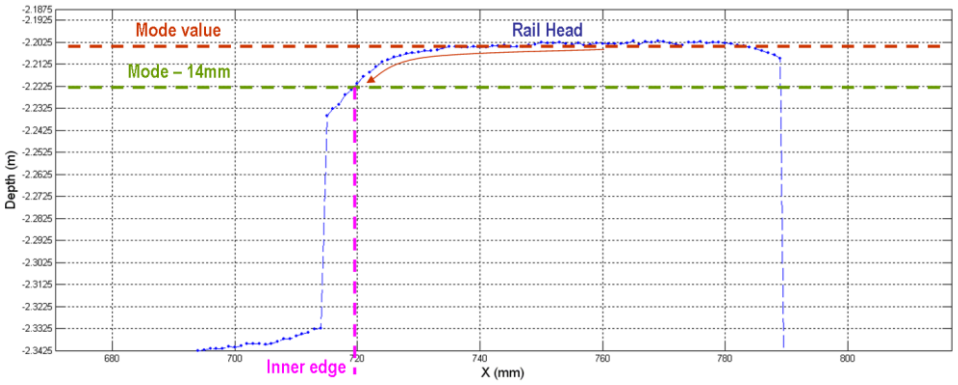

FIGURE 6 Rail head inner edges computation example (right head). A mirrored version of this procedure is applied over the left rail head.

Once the inner edges of both the right and left rail are detected for one specific scan-line, the same procedure is applied in a pre-defined number of scan-lines. According to the sensor resolution, each scan-line represents 1mm. Then, all the inner edges of the rail head are robustly modeled by means of a RANSAC-based line fitting procedure (see Figure 7). After we determine the inner rail lines, the last step is the calculation of the rail gauge between matching points. A post-processing step is applied to the estimated rail gauge curve by smoothing it with 1D 1x7 Gaussian filter.

FIGURE 7 Rail head inner lines detection examples.

Rail fasteners detection

Rail fasteners detection is carried out using a two-staged approach. First, the base plate is located using a 2D matching scheme applied over depth images directly obtained from the 3D data. Second, a 3D Iterative Closest Point (ICP) is applied using previous knowledge about the fasteners location.

Depth images are obtained by integrating the 3D information given by the laser. The gray color provided to the 2D image is directly related with the distance between the point and the laser. The location of the point is directly related with the X-Y coordinates. The maximum and minimum range used when coding the distance into a gray value is defined using previous knowledge about the sensor height. Some examples of the depth images obtained using this procedure are depicted in Figure 8. The 2D matching approach uses a pre-defined template that has to be given as a manual input. This template should contain the base plate, the rail and the fasteners. This is the unique process that requires manual intervention. Once the 2D template is given, the base plate location system applies a 2D template matching between the template and the depth image, guided by the location of the rail (which is detected following the aforementioned procedure). Two examples of the base plate location approach are showed in Figure 9. Note that in this case, two templates are used depending on the rail (left or right). A red line is showed as the detected inner edge of each one of the rails.

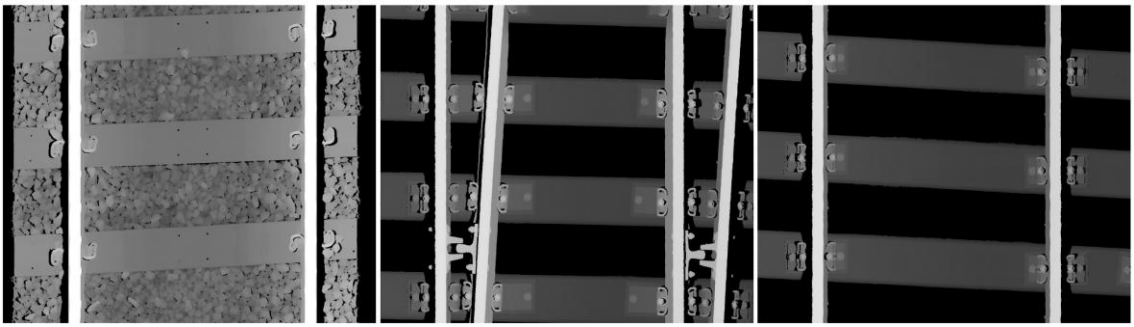

FIGURE 8 Three different depth image examples.

Once the base plate are properly located, a 3D ICP algorithm is applied, using a manually pre-defined 3D model of the fastener and previous knowledge about the expected location of the fastener. The located base plate is firstly isolated in 3D. Then, we extract the 3D cloud of points corresponding to the expected location of the fastener. Finally, we apply ICP with that cloud of points with the pre-defined 3D model. If the difference between both

cloud of points is grater than a threshold, we consider that the fasteners is missed. Some examples of this procedure are depicted in Figure 10.

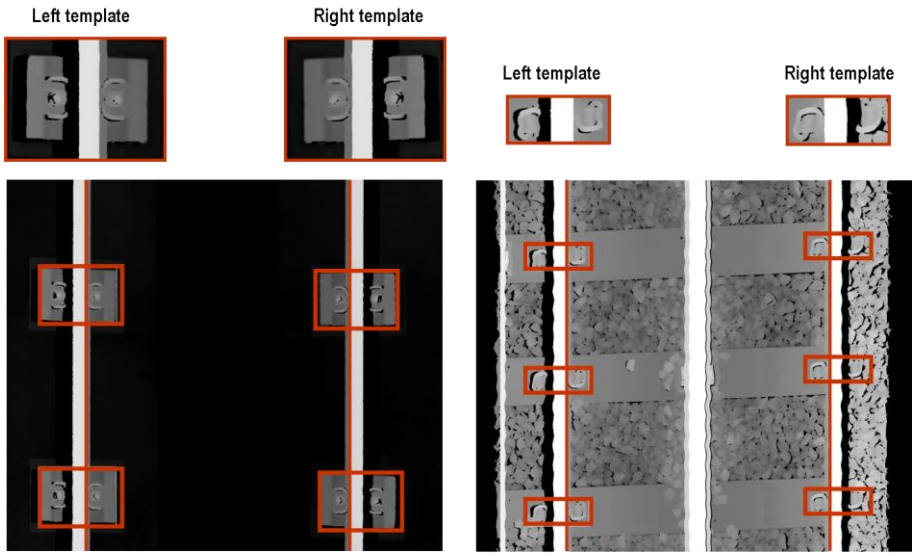

FIGURE 9 Base plate location examples. Left: tension clamp. Right: e-Clip.

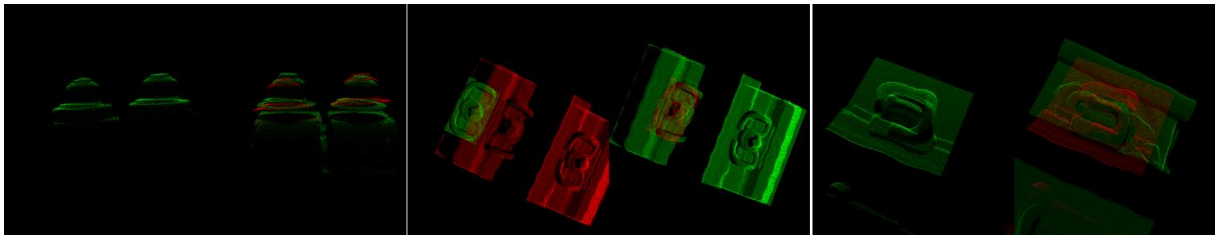

FIGURE 10 ICP examples. Left: bolt clamp. Middle: tension clamp. Right: e-Clip.

EXPERIMENTAL RESULTS

In order to validate the proposed automated rail track inspection system, we devised a set of experiments using real data obtained from Metro Madrid and London Underground. The system is firstly calibrated for rail gauge estimation using data recorded in a controlled scenario. Preliminary results are showed in the context of missing rail fasteners detection.

Calibration results

Two steel guides (see Figure 11) placed at a set of pre-defined positions in a controlled scenario are used to define a ground truth and establish a reference pattern. The rail gauge detection system is run and the results are compared with the ground truth. Table 1 shows the reported results. As we can observe, the average error is 0.9952%, always below the ground truth values. Accordingly, we correct all the rail gauge estimation by a factor of 1.009952 to obtain the best estimation. It leads to an average post-calibration error of 0.0103%.

FIGURE 11 3D reconstruction of the two steel guides used for sensor calibration.

TABLE 1 Ground truth and estimated rail gauge values.

Ground truth (mm)	Before calibration			After calibration		
	Estimated rail gauge (mm)	Error (mm)	Relative Error (%)	Estimated rail gauge (mm)	Error (mm)	Relative Error (%)
1200	1187.9	12.14	1.01	1187.9	0.28	0.02%
1300	1290.4	9.58	0.73	1290.4	-3.24	-0.25%
1400	1388.5	11.47	0.82	1388.5	-2.32	-0.17%
1500	1484.8	15.17	1.01	1484.8	0.42	0.03%
1600	1584.7	15.28	0.96	1584.7	-0.47	-0.03%
1700	1681.1	18.87	1.11	1681.1	2.17	0.13%
1800	1778.5	21.49	1.19	1778.5	3.80	0.21%
1900	1878.7	21.35	1.23	1878.7	2.60	0.14%
Average	--	15.6687	0.9952	--	**0.41**	**0.0103**

Rail gauge detection experiments

We collected a considerable amount of data corresponding to two different routes at the Metro Madrid and London Underground. A total of 840 meters were recorder from Metro Madrid whereas a total of 500 meters were collected from the London Underground. The nominal rail gauge at straight sections was 1445mm and 1435mm for Metro Madrid and London Underground respectively. Results obtained from the Madrid route are depicted in Figure 12. The route contains a section with undetected turnouts, a straight section and a curve. Note that nominal values for curve sections are always greater than for straight sections. Results obtained from the London route are supplied in Figure 13. Some spurious values were obtained due to vibrations in the recording platform.

As can be observed in both cases, the estimated rail gauges were very close to the nominal gauge. Although no ground truth values were available for the whole route, some control points were recorded with errors lower than 1mm in all cases. Accordingly, we consider that the obtained results clearly validate our rail gauge detection approach.

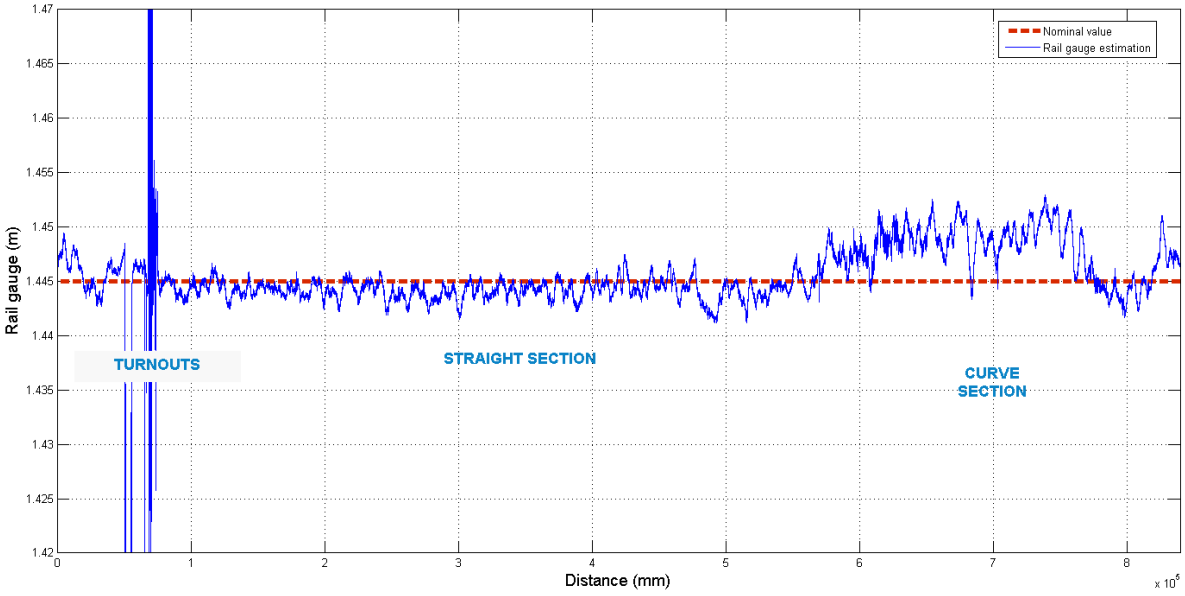

FIGURE 12 Estimated rail gauge corresponding to a section of 840m of the Metro Madrid. The section contains turnouts (non-detected), a straight section and a curve.

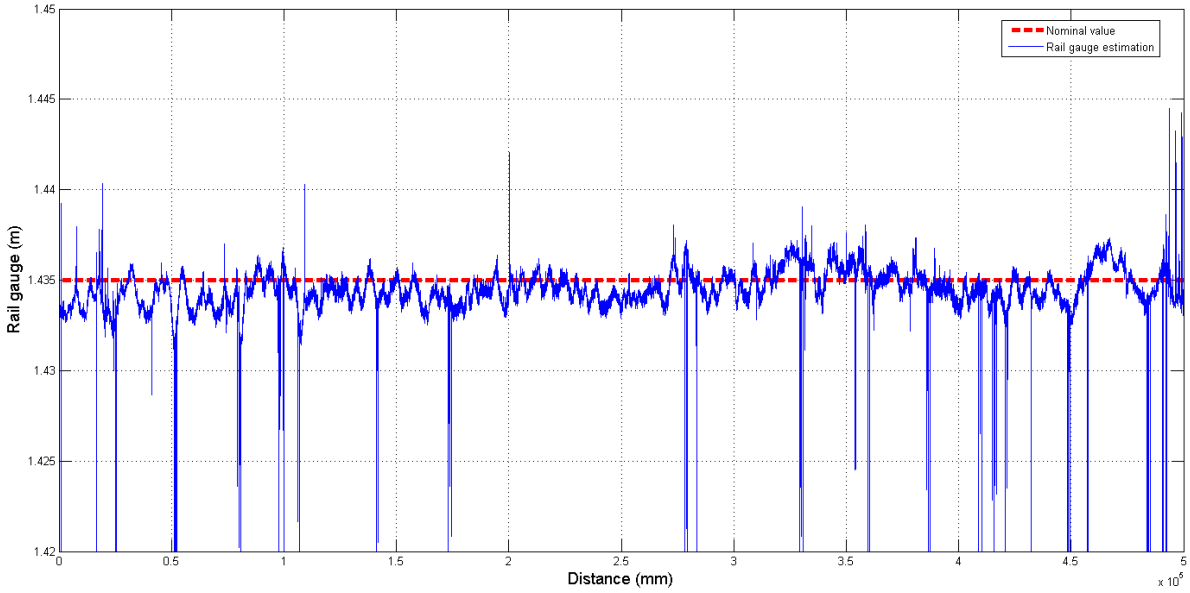

FIGURE 13 Estimated rail gauge corresponding to a section of 500m of the London metro. The section was mainly a straight section.

Rail fasteners detection experiments

The data collected from both Metro Madrid and London Underground, contains two different types of fastening systems: tension clamp (Madrid) and e-Clip (London). Unfortunately the data for both routes showed no missing components, so in practice we were only able to validate our rail fasteners detection approach in terms on false positives. No false positives were reported.

CONCLUSIONS AND FUTURE WORK

In this work a range-based rail gauge and rail fastener detection system was presented. A high-speed laser scanner that provides both 2D intensity images and high-resolution 3D profiles of the railroad track was used to capture data in an off-line fashion. Track gauge is estimated by analyzing edges on the 3D profiles of subsequent scan-lines. The Derivative of Gaussian is applied to isolate edges in the presence of noise. The inner edges of both rails are estimated 14mm below the rail head surface. Then inner lines are robustly estimated using a 3D RANSAC-based line estimator. The base plates that support the rail fastening system are firstly located by means of a 2D template matching technique applied over 2D depth images. Then, rail fasteners are detected by means of a 3D Iterative Closest Point approach. Results were presented from two different scenarios: Metro Madrid metro and London Underground.

Future works should include the detection of turnouts. Some improvements can be introduced in the rail gauge fastener detection procedure using 2D/3D pattern recognition techniques. Other potential defects such as rail cracks or rail burns will be considered in future versions of the system. Finally, more experimental work has to be carried out, using different routes of thousands of meters with the corresponding ground truth obtained by a manual labeling process. Thus, we would be able to validate the whole system for being commercially exploited.

ACKNOWLEDGMENTS

The authors would like to acknowledge the local authorities of both Metro Madrid and London Underground, for their valuable support. This work was supported by Euroconsult Group (Madrid, Spain) through an interdisciplinary research collaboration with the Innovative Sensing and Intelligent Systems (ISIS) research group at the University of Alcalá (UAH, Alcalá de Henares, Spain).

REFERENCES

(1) http://safetydata.fra.dot.gov/OfficeofSafety/

(2) Vojtech EKSLER. Intermediate report on the development of railway safety in the European Union. European Railway Agency. Safety Unit, May 2013.

(3) Sawadisavi, S., Edwards, J.R., Hart, J.M., Resendiz, E., Barkan, C.P.L., Ahuja, N., "Machine-Vision Inspection of Railroad Track," 2008 AREMA Conference Proceedings, American Railway and Maitenance of Way Association (AREMA), Landover, Maryland.

(4) Edwards, J., Hart, J., Sawadisavi, S., Resendiz, E., Barkan, C., Ahuja, N. "Advancements in railroad track inspection using machine vision technology," AREMA Conference Proceedings on American Railway and Maintenance of Way Association, 2009.

(5) Molina, L., Resendiz, E., Edwards, J., Hart, J., Barkan, C., Ahuja, N. "Condition monitoring of railway turnouts and other track components using machine vision," in Proc. Transportation Research Board 90th Annual Meeting, Washington, DC, 2011.

(6) Resendiz, E., Hart, J., Ahuja, N. "Automated Visual Inspection of Railroads Tracks". IEEE Transactions on Intelligent Transportation Systems, Vol. 14, No. 2, 2013.

(7) Li, Y., Otto, C., Haas, N., Fujiki, Y., Pankanti S. "Component-based track inspection using machine-vision technology". In Proceedings of the 1st ACM International Conference on Multimedia Retrieval ICMR, 2011.

(8) Trinh, H., Haas, N., Ying, Li., Otto, C., Pankanti, S. "Enhanced rail component detection and consolidation for rail track inspection". IEEE Workshop on Applications of Computer Vision (WACV), 2012.

(9) Babenko, P. "Visual Inspection of Railroad Tracks". Ph.D dissertation, University of Central Florida, Fall 2009.

(10) Shah, M. "Automated Visual Inspection/Detection of Railroad Track". Final report. Contract No: BD550, RPWO #8. University of Central Florida. July 2010.

(11) AURORA, Georgetown Rail Equipment Company. *http://www.auroratrackinspection.com*. Accessed in June 2013.

(12) ENSCO, Track Inspection Vehicles and Systems, *http://www.ensco.com/products-services/rail-technologies/track-inspection-systems.htm.* Accessed in June 2013.

(13) MERMEC Group, Diagnostic Solutions, *http://www.mermecgroup.com/15/1/diagnostic-solutions.php*, Accessed in June 2013.

(14) RailVision, TrackVuew, *http://www.rail-vision.co.uk/node/41*, Accessed in June 2013.

(15) Pavemetrics, Laser Tunnel Scanning System, *http://www.pavemetrics.com/en/ltss.html*, Accessed in June 2013.